MODELLING THE FLOW IN AN EXPERIMENTAL FLUME WITH SUBMERGED RIGID CYLINDRICAL VEGETATION ELEMENTS

Anastasios Stamou[1], Georgia Papadonikolaki[1], & Anthi Gkesouli[1]

[1]Department of Water Resources and Environmental Engineering,
National Technical University of Athens (NTUA), Iroon Polytechniou 5, 15780 Athens, Greece.
E-mail: stamou@central.ntua.gr

Abstract

Preliminary 3-D calculations were performed to model the flow in an experimental flume with submerged rigid cylindrical vegetation using a CFD code that employs the Scale Adaptive Simulation (SAS) concept. From the comparison of the calculations with experiments and LES calculations the following conclusions are drawn: (1) SAS calculations are encouraging; they reproduce the experimental two-layer flow that consists of the vegetation layer and the surface layer with an inflection point at the interface and they reveal all main recirculation areas that were identified in the LES computations; (2) experimental time averaged streamwise velocities are well predicted by SAS in the surface layer; however, they are overestimated in the vegetation layer, between and in front of the cylinders. Calculated vertical velocities show a more uniform distribution in the vertical direction compared to experiments; in the surface layer the agreement of vertical velocities with measurements is generally satisfactory; (3) calculated turbulence intensities show a satisfactory qualitative agreement with experimental data; horizontal values are well predicted in the surface layer and in the regions of free flow of the vegetation layer. However, in the vegetation layer experimental values are underestimated; this underestimation is more pronounced in the vertical direction.

Introduction

Flows during flood events in floodplains and wetlands are of significant ecological importance; they depend on various parameters including discharge, water level fluctuations, vegetation characteristics (arrangement, type and density) and topography. The task of modeling such flows is indeed an ambitious challenge with a possible "ultimate goal" to formulate a CFD model that (1) describes realistically the basic geometrical characteristics of the vegetation (including branches and leaves) and (2) calculates the average and temporary (e.g. turbulent) flow characteristics with acceptable accuracy, within reasonable computational time. The project "Computational research of the influence of the vegetation on the flow during floods events" that is performed in the NTUA can be considered as a preliminary attempt towards this goal. We started this project by performing a literature review on the available relevant experimental and computational studies. Taking into account the complicated 3-D geometry of the flow, we performed preliminary 3-D computations using the Reynolds Averaged Navier Stokes (RANS) equations. RANS equations have formed the basis for CFD analysis of engineering flows for many years and have been used in various cases to model vegetated flow; see for example Klopstra et al. (1997) and Lopez and Garcia (2001). RANS calculations were not satisfactory (Stamou et al., 2011) and their discrepancies with experimental data were mainly due to flow instabilities past the vegetation elements. This behavior guided us to use the unsteady RANS (URANS) equations. URANS have already been applied in flows both past a single cylinder (Young and Ooi, 2007) or a series of cylinders representing vegetation elements; however, with limited success. We verified this statement by performing some indicative computations. At this point two alternative CFD approaches were theoretically available: (1) the accurate methods of Direct Numerical Eddy Simulation (DNS) or Large Eddy Simulation (LES) and (2) the hybrid approaches, such as the Scale Adaptive Simulation (SAS) and Detached Eddy Simulation (DES).

LES has indeed shown a very good performance in calculating channel flow past a cylinder (Young and Ooi, 2007) or in a series of submerged cylinders (Stoesser et al. 2006 and 2009) and eventually is the future CFD tool towards the "ultimate goal". However, LES requires an enormous computational storage, power and CPU time, even for small calculation regions. For example Stoesser et al. (2009) used a total of approximately 113×10^6 grid points to simulate quite satisfactorily the turbulent flow in a rectangular part of the experimental channel of Liu et al. (2008) with submerged cylindrical vegetation elements that had dimensions length × width × depth equal to 0.254 m × 0.127 m × 0.1141 m. Hybrid approaches that are sometimes characterized as "snazzy" have been proven successful in certain types of flows; for example SST (Menter, 1993) to simulate buoyant air flows in indoor environments (Stamou and Katsiris, 2007). The SAS concept (Menter and Egorov,

2006) that is based on the introduction of the von Karman length-scale (L_{vK}) into the scale-determining equation of URANS turbulence models; L_{vK} allows the turbulence model to recognize resolved scales in unstable flows and to adjust the eddy-viscosity to a level, which allows the formation of a turbulent spectrum. At the same time, stable flow regions, such as attached boundary layers, are automatically treated in URANS mode. Virtually, the SAS method is an improved URANS formulation, with the ability to adapt the length scale to resolved turbulent structures. In order for the SAS method to produce a resolved turbulent spectrum, the underlying turbulence model has to go unsteady. This is typically the case for flows with a global instability, such as for flows with vortex interactions past a cylinder or past vegetation elements.

In this paper we present some preliminary SAS calculations in a flow domain with submerged cylinders representing vegetation elements; this domain, which is a part of the rectangular experimental channel for which time averaged velocities and turbulence intensities are available, was also calculated by Stoesser et al. (2009) using LES. Indicative calculations for the flow past a single cylinder are also briefly presented.

The Numerical Code

Calculations were performed with the numerical code CFX-13.0 (http://www.ANSYS.com) that uses the finite volume method for the spatial discretisation of the domain. The equations of the model are integrated over each control volume, such that the relevant quantity (mass, momentum and turbulence characteristics) is conserved, in a discrete sense. For the continuity equation (pressure-velocity coupling), high resolution approximation is used. The second order backward Euler scheme approximates the transient term. A scalable and fully implicit coupled solver is used for the solution of the equations.

Calculations past a cylinder

The flow past a cylinder is one of the most documented benchmarks in the literature since it combines a simple geometry with a complex flow regime that varies significantly with Reynolds number. Vegetation is widely simulated by submerged cylindrical elements that in the majority of the cases are assumed to be rigid. We performed our first SAS calculations for this flow at a Reynolds number $Re_D = U_\infty D/\nu = 3900$, where D=0.10 m is the diameter of the cylinder, U_∞=0.0429 m/s is the free stream velocity and $\nu = 1.1 \times 10^{-6}$ m^2/s is the viscosity of the water. Calculations were compared against the experimental data of Ong and Wallace (1996), Lourenco and Shih (1993), Norberg (1994), Cardell (1993) and LES calculations (Young and Ooi, 2007) with 4.32×10^6 grid points. In this work some indicative information and results are presented; more information can be found in Stamou and Papadonikolaki (2012). The computational domain was rectangular, extending 10D upstream, 20D downstream and 11D in the crossflow direction; the spanwise dimension was 1D. The computational grid was unstructured and consisted of 1.47×10^6 control volumes; in the vicinity of the cylinder the grid was refined, as shown in Figure 1.

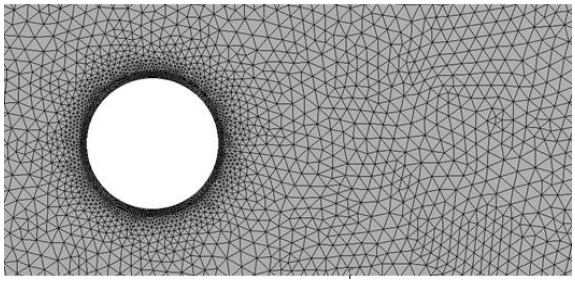

Figure 1: Refinement of the grid near the cylinder

Figures 2 and 3 present the mean streamwise velocity (U) values along the center line, aft of the cylinder, and profiles in the wake of the cylinder, respectively. Table 1 summarizes the calculated average values of important non-dimensional flow parameters that are the base pressure coefficient ($\bar{C}_{Pb}$), the mean drag coefficient ($\bar{C}_{Pb}$), the Strouhal number (S_t), and the non-dimensional size of the recirculation region (L_r/D); $\bar{C}_{Pb}$ is a good indicator of whether the predicted pressure in the wake is correct and therefore whether the overall drag will be correct.

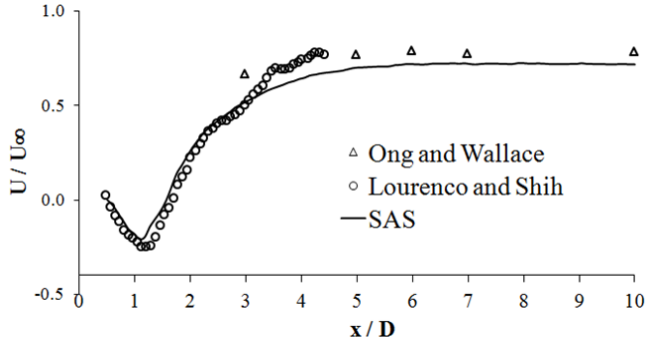

Figure 2: Streamwise velocity on the center line

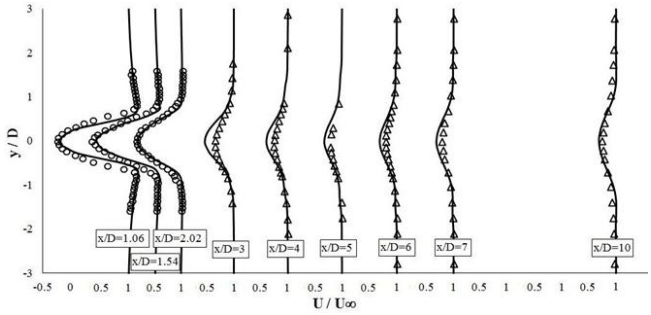

Figure 3: Calculated streamwise velocities in the wake of the circular cylinder; Lourenco and Shih (1993) are denoted by ○ and Ong and Wallace (1996) are denoted by ∆

Table 1: Overall flow parameters

Case	Experiments	SAS	LES
$\bar{C}_D$	0.99 ± 0.05	0.90	1.03
$-\bar{C}_{Pb}$	0.88 ± 0.05	0.93	0.908
S_t	0.215 ± 0.005	0.23	0.212
L_r/D	1.4 ± 0.1	1.4	-

Generally, calculations are in satisfactory agreement with measurements. Streamwise velocities are well predicted near the cylinder; however, they are underestimated at distances x greater than 3D. Turbulence intensities showed also a satisfactory agreement with experimental data (Stamou and Papadonikolaki, 2012).

Computational details

The computational domain that is shown in Figure 4 is a part of the rectangular experimental channel of Liu et al. (2008); the six verticals at which measurements were taken are also shown in Figure 4 and numbered from 1 to 6. This domain was used in the LES computations by Stoesser et al. (2009). The channel has a water depth equal to h=0.1141 m and includes 16 rigid submerged cylinders of diameter D=0.00635 m and height h_p=0.076 m (h/h_p=1.50, $h_p/D\approx12$ and $h/D\approx18$) in a staggered arrangement. The dimensions of the domain are equal to 40D, 20D and 18D (equal to h) in the x (horizontal-streamwise), y (spanwise) and z (vertical) direction, respectively.

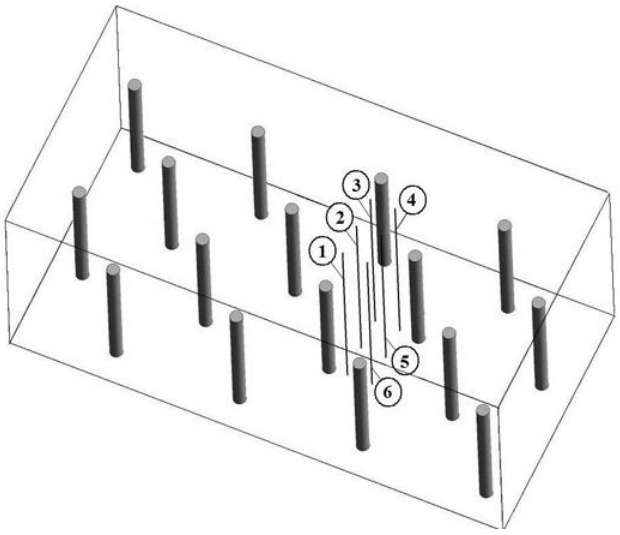

Figure 4: Computational domain with the six verticals where measurements were taken

A relatively coarse unstructured computational grid was used in the computations consisting of 1.15×10^6 control volumes; the minimum edge size of the grid elements was 0.001 m and the maximum was 0.050 mm, close to the free surface. Figure 5 shows a horizontal plane of the grid at height equal to z=D indicating the refinement of the grid in the regions of the cylinders.

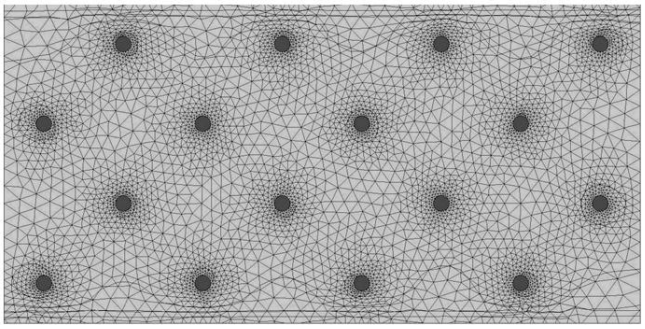

Figure 5: Horizontal plane of the numerical grid at z=D

In the x direction a periodic boundary condition was employed between the inlet and outlet boundaries assuming a constant flow rate equal to 0.0047 m^3/s that corresponds to a bulk average velocity equal to U_b=0.3272 m/s. Periodicity was also employed in the y direction. At the channel bed the no-slip condition was applied and the free surface was considered as a frictionless rigid lid and treated as a plane of symmetry. The cylinders were assumed to be smooth.

We started our computations using the SST model until steady state; then, we continued with SAS computations for approximately 20 flow through times T, where $T=L_x/U_b$=78 s, to establish fully developed turbulent flow (Stoesser et. al., 2009). After this transitional period, we performed computations for another 20 T during which we determined the average and turbulent flow characteristics.

Results and Discussion

Layered flow

In Figure 6 and 7 the time-averaged, normalized (with U_b) streamwise (U) and vertical (W) velocities are shown together with the experimental data of Liu et al. (2008) and the LES computations of Stoesser et al. (2009).

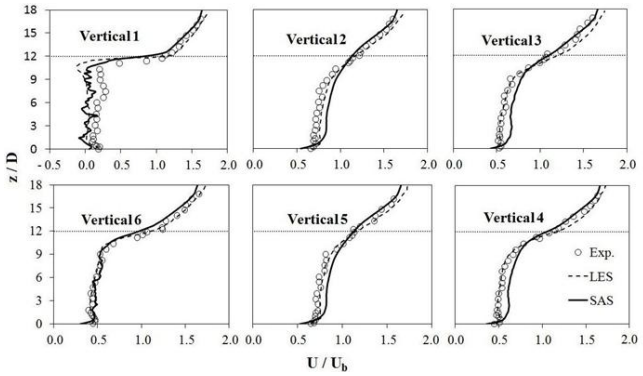

Figure 6: Comparison of calculated streamwise velocities with measurements and LES computations

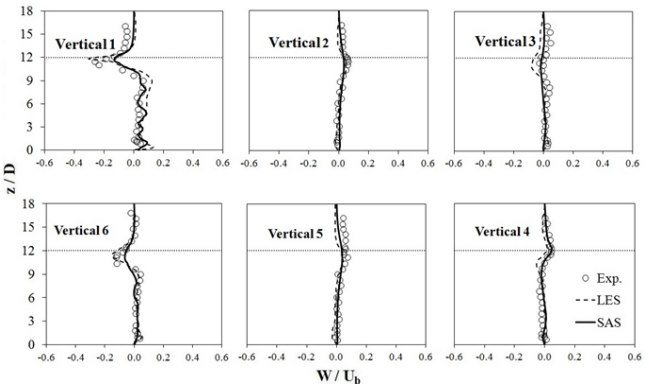

Figure 7: Comparison of calculated vertical velocities with measurements and LES computations

Figures 6 and 7 verify the "two-layer approach" that has been applied by many researchers; see for example Klopstra et. al. (1997), Van Helzen (1999) and Defina and Bixio (2005). This approach divides the average flow domain into two layers that are separated via an "interface", (1) the first within the vegetation called "vegetation layer" and (2) the second above the first it called the "surface later".

In the vegetation layer the flow decelerates; Figure 6 shows that velocity profiles are very similar almost throughout the entire width of the channel with the streamwise velocities being slightly higher in the free stream areas (verticals 2 and 5), with the exception of the recirculation areas behind the cylinders (verticals 1 and 6) that extend from the bed to the top of the cylinders. The streamwise velocity profile in the vicinity of the vegetation resembles to a mixing layer profile and exhibites an inflection point at $z=h_p$.

In the surface layer the flow accelerates, causing a strong shear layer in the region of interface; streamwise velocity profiles are similar throughout the entire width of the channel.

SAS calculations show a satisfactory agreement with experimental data. Streamwise velocities are very well predicted in the surface layer; however, in the vegetation layer Figure 6 shows that they are overestimated in the regions of free flow (verticals 2 and 5) and in front of the cylinders (verticals 3 and 4). Calculated vertical velocities show a more uniform distribution in the vertical direction compared to experiments; in the surface layer the agreement of vertical velocities with experiments is generally satisfactory. The above mentioned discrepancies of the SAS calculations with experiments can be attributed to the relatively coarse grid used in the calculations and the short averaging time (20T) to derive average velocity values. As expected, LES calculations show a better agreement with experiments than SAS calculations; it is noted that in the LES calculations an averaging time of 50T has been used.

Flow separations and instabilities

The cylinders act as solid impermeable bodies and the establishing flow will resemble classical wake-flows that are characterized by steep velocity gradients and flow separation at the boundaries. Numerous studies have investigated wake flows around vertical cylindrical elements, and revealed details of the flow (Hunt et al., 1978; Zdravkovich, 1997).

The approaching flow is deflected downward to initiate horseshoe vortex systems (recirculation regions with reduced velocities and stresses) at the channel bed as shown in Figure 8; moreover, alternating roller-type vortices are shed from the separation points. High momentum water from free stream areas is sucked into these systems and then it is transported upwards, as also shown in Figure 7 (positive vertical velocities in verticals 1 and 6), in a spiraling motion. This motion that is shown in Figure 9a and c extends from the bed (z=0) until approximately z=11D (i.e. 1D below the top of the cylinders) and results in the increase of the size of the recirculation regions with height; this size was estimated equal to 1D at z=0 and 1.3D at z=11D. Moreover, Figure 9b denotes that flow separation occurs at the top of the cylinders resulting in the formation of small recirculation regions with trailing (or tip) vortices. These vortices support the downward motion in the region of interface of the water of the surface layer; this motion is also evident in vertical 1 of Figure 7, where relatively high negative vertical velocities are observed. Firstly, water of the surface layer is entrained in the wake and then towards the vegetation layer. Due to continuity, in free stream regions water is transported upwards towards the surface layer, noted also in verticals 2, 3, 4 and 5 of Figure 7, where positive vertical velocities are observed near the interface.

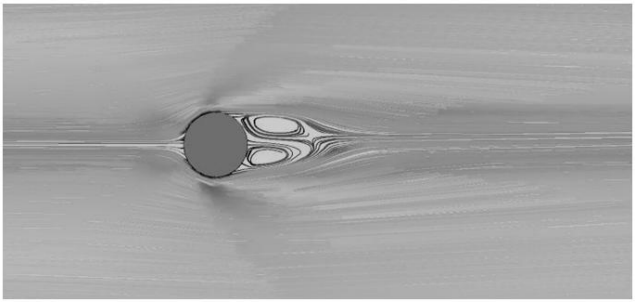

Figure 8: Horseshoe vortex at the bed of the channel

Turbulence characteristics

In Figures 10 and 11 contours of time-averaged streamwise (U') and vertical turbulence intensities (W') are shown, respectively, at two longitudinal (xz) planes called xz-16 and xz-25; xz-16 passes through verticals 1 and 6, and xz-25 passes through verticals 2 and 5.

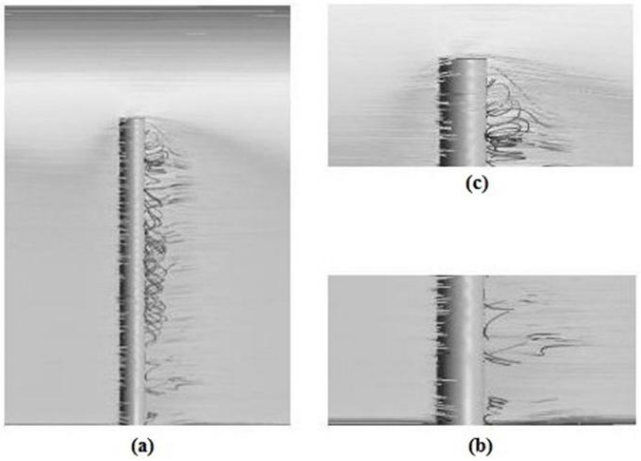

Figure 9: Spiraling motion behind the cylinder (a and b) and small recirculation in the top of the cylinder (c)

In Figures 12 and 13 streamwise and vertical turbulence intensities are shown, respectively, together with the experimental data of Liu et al. (2008) and the LES computations of Stoesser et al. (2009); these values are normalized with the shear velocity $U_*=(ghS)^{0.5}=0.05795$ m/s, where S=0.003 is the slope of the energy line.

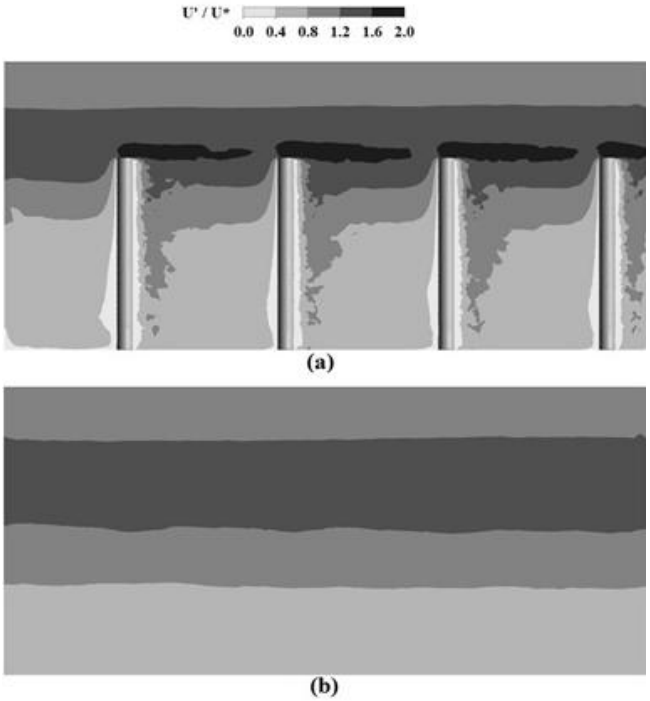

Figure 10.Contours of U'/U_* at planes (a) xz-16 and (b) xz-25

Figures 10 to 13 show that high levels of turbulence are observed (1) near the interface shear layer, (2) in the recirculation regions behind the cylinders (due to the von Karman vortices of the instantaneous flow) and (3) in the regions of tip vortices, on the top of the cylinders.

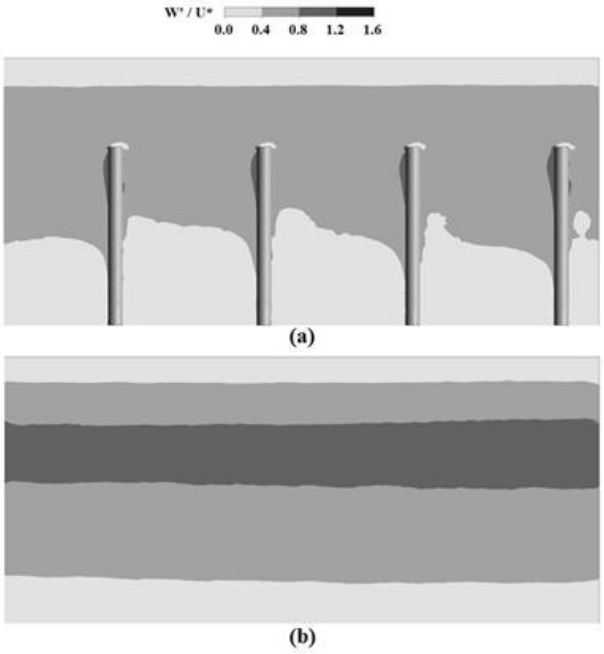

Figure 11.Contours of W'/U_* at planes (a) xz-16 and (b) xz-25

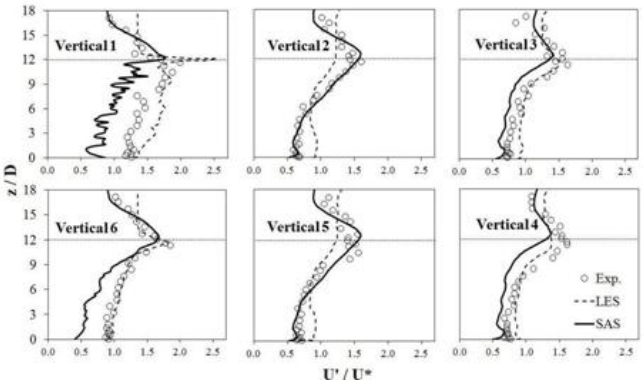

Figure 12: Comparison of calculated U'/U_* with measurements and LES computations

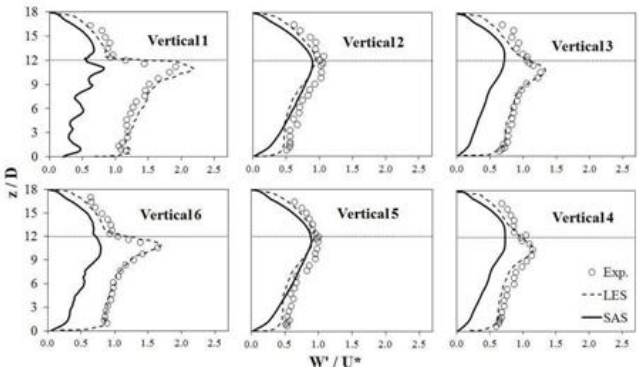

Figure 13: Comparison of calculated W'/U_* with measurements and LES computations

The shear layer at the interface is very strong generating originally U' that are redistributed to W' resulting in very high vertical mass and momentum exchange. Indeed, Figure 12 indicates that peak values of U'/U_* are found at the interface (i.e. at the velocity inflection), while peak values of V'/U_* are observed at a lower level (z/D=11) due

to downward motion of water supported by the tip vortices penetrating into the vegetation layer. Moreover, Figure 11a shows that high values of W' are also observed in front of the cylinders close to their top; these are due to the splatting effect that was noted by Stoesser et al. (2009), according to which the flow impinges on the cylinders and U' is redirected to V' and W'. Generally, SAS calculations show a satisfactory qualitative agreement with experimental data. U' values are well predicted in the surface layer and in the regions of free flow of the vegetation layer (verticals 2 and 5); surprisingly, SAS shows a better agreement than LES calculations. However, in the vegetation layer U' values are underestimated both in front (verticals 3 and 4) and behind the cylinders (verticals 1 and 6); in these locations a more pronounced underestimation in the values of W' is observed that includes the underestimation of the splatting effect; see Figure 10 verticals 3 and 4. Again, the coarse grid and the short averaging time can again be the reasons for the above mentioned discrepancies.

Conclusions

Preliminary SAS calculations have been performed in a computational domain with submerged cylindrical vegetation elements using a relatively coarse grid of 1.15 million finite volumes and averaging time of approximately twenty flow through times for the determination of turbulent quantities. From the comparison of the calculations with experiments and LES calculations the following conclusions are drawn: (1) SAS calculations are encouraging; they reproduce the experimental two-layer flow that consists of the vegetation layer and the surface layer with an inflection point at the interface and they reveal all main recirculation areas that were identified in the LES computations; (2) experimental time averaged stream-wise velocities are well predicted by SAS in the surface layer; however, they are overestimated in the vegetation layer, between and in front of the cylinders. Calculated vertical velocities show a more uniform distribution in the vertical direction compared to experiments; in the surface layer the agreement of vertical velocities with measurements is generally satisfactory; (3) calculated turbulence intensities show a satisfactory qualitative agreement with experimental data; horizontal values are well predicted in the surface layer and in the regions of free flow of the vegetation layer. However, in the vegetation layer experimental values are underestimated; this underestimation is more pronounced in the vertical direction. Discrepancies with experiments were attributed to the coarse grid and the short averaging time used in the computations. Computations with finer grids and averaging times of approximately 50 flow through times are currently underway and will be presented in a future publication.

Acknowledgments

The present work was performed within the framework of the Program for Basic Research (PEVE-2010) of the National Technical University of Athens entitled "Computational research of the influence of the vegetation on the flow during floods events".

References

ANSYS-CFX, Release 13.0, URL: http://www.ANSYS.com.

Cardell, G. S. (1993). *Flow past a circular cylinder with a permeable splitter plate*. Ph.D. thesis, Graduate Aeronautical Laboratories, California Institute of Technology.

Defina, A., & Bixio, C. (2005). Mean flow and turbulence in vegetated open channel flow. *Water Resources Research*, 41, pp. 1-12.

Hunt, J. C. R., Abell, C. J., Peterka, J. A., & Woo, H. (1978). Kinematical studies of flows around free or surface–mounted obstacles – applying topology to flow visualization. *Journal of Fluid Mechanics*, 86 (1), pp. 179–200.

Klopstra, D., Barneveld, H.J., van Noortwijk, J.M., & van Velzen, E.H. (1997). Analytical Model for Hydraulic Resistance of Submerged Vegetation. Managing Water: Coping with scarcity and abundance, *Proceedings of the 27th IAHR Congress*, San Fransisco, pp. 775-780.

Liu, D., Diplas, P., Fairbanks, J.D, Hodges, C.C. (2008). An experimental study of flow through rigid vegetation. *Journal of Geophysical Research and Earth Sciences*, 113, pp. 1–16.

Lopez, F., & Garcia, M. (2001). Mean flow and turbulence structure of open-channel flow through non-emergent vegetation. *Hydraulic Engineering*, ASCE, 127, pp. 392-402.

Lourenco, L. M., & Shih, C. (1993). Characteristics of the plane turbulent near wake of a circular cylinder: A particle image velocimetry study. *Fluids*, 9, pp. 223-253.

Menter, F. R. (1993). Zonal Two Equation k-ω Turbulence Models for Aerodynamic Flows. *AIAA*, Paper 93-2906.

Menter, F., & Egorov, Y. (2006). SAS Turbulence Modelling of Technical Flows. *Direct and Large-Eddy Simulation*, VI (Part XV), pp. 687-694.

Norberg, C. (1994). An experimental investigation of the flow around a circular cylinder: influence of aspect ratio. *Journal of Fluid Mechanics*, 258, pp. 287-316.

Ong, L., & Wallace, J. (1996). The velocity field of the turbulent very near wake of a circular cylinder. *Experiments in Fluids*, 20, pp. 441-453.

Stamou, A., & Katsiris, I. (2006). Verification and Application of a CFD Model for the Evaluation of Thermal Comfort in Office Spaces. *Building and Environment*, 41, pp. 1171-1181.

Stamou, A.I., & Papadonikolaki, G. (2012). Assesment of SAS calculations for flow over a cylinder at Reynolds of 3900. (in preparation).

Stamou A. I., Papadonikolaki G., Gkesouli A. and Nikoletopoulos A. (2011). Modeling the effect of vegetation on river floodplain hydraulics. *12th International Conference on Environmental Science and Technology (CEST2011)*, Rhodes island, Greece.

Stoesser, T., Liang, C., Rodi,W., Jirka, G.H. (2006). Large eddy simulation of fully-developed turbulent flow through submerged vegetation. *Proceedings of River Flow 2006, 3rd International Conference on Fluvial Hydraulics*, Lisbon, Portugal.

Stroesser, T., Salvador, G. P., Rodi, W., & Diplas, P. (2009). Large Eddy Simulation of Turbulent Flow Through Submerged Vegetation. *Transport in Porous Media*, 78 (No.3), pp. 347-365.

Young, M. E., & Ooi, A. (2007). Comparative assesment of LES and URANS for flow over a cylinder at Reynolds of 3900. *16th Australian Fluid Mechanics Conference*, Gold Coast, Australia.

Zdravkovic, M. M. (1997). *Flow around circular cylinders, Vol 1: Fundamentals*. Oxford University Press Inc., Oxford.